Langmuir

ARTICLE

pubs.acs.org/Langmuir

Hollow Nanospheres Based on the Self-Assembly of Alginate-*graft*-poly(ethylene glycol) and α-Cyclodextrin

Xian-Wei Meng,[†,‡] Wei Ha,[‡] Cong Cheng,[†] Zhen-Qiang Dong,[†] Li-Sheng Ding,[†] Bang-Jing Li,[*,‡] and Sheng Zhang[*,†]

[†]State Key Laboratory of Polymer Materials Engineering, Polymer Research Institute of Sichuan University, Sichuan University, Chengdu 610065, China

[‡]Key Laboratory of Mountain Ecological Restoration and Bioresource Utilization, Chengdu Institute of Biology, Chinese Academy of Sciences, Chengdu 610041, China

Supporting Information

ABSTRACT:

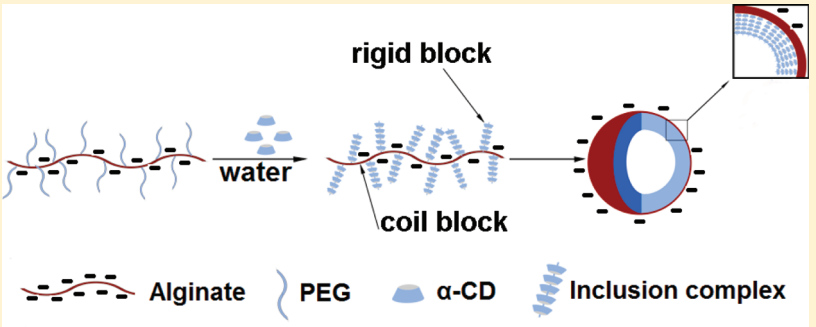

This article studies the self-assembly of alginate-*graft*-poly(ethylene glycol) (Alg-*g*-PEG) and α-cyclodextrin (α-CD) in aqueous solution. It was found that they could form hollow spheres because of the formation of coil−rod Alg-*g*-PEG/α-CD inclusion complexes. In these Alg-*g*-PEG/α-CD complexes, the α-CDs are stacked along the PEG side chains to form a rod block, and alginate main chains act as a coil block. More rod-like blocks in Alg-*g*-PEG/α-CD favor the formation of small assemblies. The assemblies of Alg-*g*-PEG/α-CD show a dependence on concentration, temperature, pH, and salt concentration. At low concentration (below 0.125%) or high temperature (above 32 °C), Alg-*g*-PEG/α-CD particles were unstable and disrupted. Increasing the salt or decreasing the pH resulted in the aggregation of Alg-*g*-mPEG/α-CD particles, as detected by the increase in the recorded hydrodynamic diameter (D_h).

1. INTRODUCTION

Polymeric hollow spheres with nano- or submicrometer dimensions have been attracting increasing interest because of their potential applications in many fields such as microreactors, controlled delivery, and the development of artificial cells.[1−3] Because of their hollow core structure, such polymeric spheres can encapsulate large quantities of guest molecules or large guests within the empty domain. Hollow spheres could be obtained by different approaches, such as emulsion polymerization, the use core−shell micelles made of block copolymers, noncovalently connected micelles, or a template method.[4−13] However, these strategies require the core to be removed in order to creat a hollow interior. Since Jenekhe and Chen reported that rigid-coil copolymers could self-assemble to hollow spheres directly in their selective solvent,[14,15] the self-assembly of the rigid-coil system has become one of the most important approaches to building hollow spheres. For example, Jiang reported that a hydrogen-bonding complex combining rod-like and coil-like polymers could also self-assemble to hollow spheres directly.[16−20] However, these self-assembled hollow spheres lack biocompatibility and nonbiodegradability because the rod-like blocks are π-conjugated long chains.

In a previous article, we reported briefly on a novel approach to constructing hollow spheres by the inclusion of alginate-*graft*-poly(ethylene glycol) (Alg-*g*-PEG) and α-cyclodextrin (α-CD), in which the rigid blocks are formed by self-assemblyed α-CD with poly(ethylene glycol) (PEG).[21] Further research has proven that these Alg-*g*-PEG/α-CD hollow spheres could serve as an good alternative to enzyme encapsulation because of their good biocompatibility.[22] An understanding of the relation between the physical properties and the environmental conditions not only is of academic interest but also is very important to such applications. The purpose of this article is to describe the preparation and properties of Alg-*g*-PEG/α-CD hollow spheres in detail and

Received: January 3, 2011
Revised: October 14, 2011
Published: October 17, 2011

Scheme 1. Synthesis of Alg-*g*-PEG

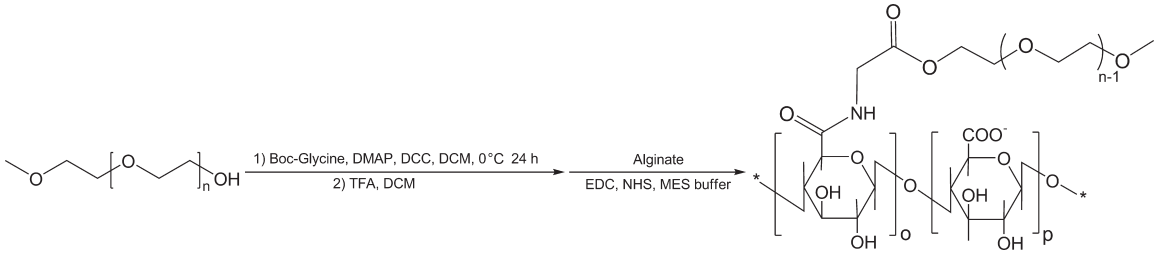

discuss their dependence on temperature, concentration, pH, and salt concentration.

2. EXPERIMENTS

2.1. Materials. Methoxypoly(ethylene glycol) (CH_3OPEG) (M_n = 2000) and *N-tert*-butoxycarbonylglycine (N-*t*-Boc-glycine) were purchased from Aldrich Chemical Co. and dried in vacuum at 40 °C for 24 h before use. 4-(Dimethylamino) pyridine (DMAP), dicyclohexylcarbodiimide (DCC), morpholinoethanesulfonic acid (MES), 1-ethyl-3-[3-(dimethylamino)propyl] carbodiimide hydrochloride (EDC), and *N*-hydroxysuccinimide (NHS) were local commercial products that were used as received.

2.2. Synthesis. The syntheses procedures of the products are listed in Scheme 1.

2.2.1. CH_3OPEG-CH_2CH_2NH-Boc. CH_3OPEG-CH_2CH_2NH-Boc was synthesized according to the method of Eiselt et al.[12] CH_3OPEG (2.5 mmol), *N-t*-Boc-glycine (5.5 mmol), and DMAP were added to a CH_2Cl_2 solution (30 mL). Subsequently, DCC (6 mmol) was added, followed by stirring for 24 h at 0 °C. After removing dicyclohexylurea (DCU) by filtration, the filtrate was concentrated in vacuum at room temperature. The resultant was dissolved in a minimal amount of acetone and cooled overnight, and the precipitated DCU was filtered off. After the solvent was evaporated, the product was obtained by drying under vacuum at room temperature for 24 h. ^{1}H NMR (600 MHz, $CDCl_3$, δ): 1.45 (s, 9H, CH_3), 3.38 (s, 3H, CH_3), 3.64 (s, 50H, CH_2), 3.82 (t, 2H, CH_2), 3.94 (d, 2H, CH_2), 4.30 (t, 2H, CH_2), 5.12 (s. 1H, NH). The ^{1}H NMR spectrum of CH_3OPEG-CH_2CH_2NH-Boc is shown in Figure S1 in the Supporting Information.

2.2.2. CH_3OPEG-NH_2. For the removal of the *t*-Boc group, CH_3O-PEG-CH_2CH_2NH-Boc was dissolved in a mixture of CH_2Cl_2/THF (1/1 v/v). The reaction mixture was stirred for 2 h at 0 °C and then evaporated to dryness. The deprotected derivative (CH_3OPEG-NH_2) was dissolved in a NaCl solution (15%), and the pH was adjusted to 5. The filtrate was extracted three times with chloroform; the organic phases were combined and dried over Na_2SO_4. After Na_2SO_4 was filtered and the solvent was evaporated, the oil residue was dried under vacuum over P_2O_5 at room temperature for 24 h. ^{1}H NMR (600 MHz, $CDCl_3$, δ): 3.33 (s, 3H, CH_3), 2.47−3.72 (m, 52H, CH_2), 3.90 (s, 2H, CH_2), 4.32 (t, 2H, CH_2). The ^{1}H NMR spectrum of CH_3OPEG-NH_2 is shown in Figure S2.

2.2.3. Alg-g-PEG. CH_3OPEG-NH_2 was grafted onto sodium alginate according to the procedure of Eiselt et al.[23] A sodium alginate solution (1% w/v) was prepared in a buffer solution of MES (0.1 M) and NaCl (0.5 M), and the pH was adjusted to 6. Samples of NHS (292.2 mg) and EDC (98.8 mg, EDC/NHS/COO^- 1:0.5:1 mol/mol/mol) were added to the alginate solution (100 mL) to activate the carboxylic acid groups on the polymer backbone. The solution was agitated to obtain a homogeneous solution, followed by the addition of PEG solution (2% w/v). The reaction was carried out at room temperature for 10 h. The resulting mixture was dialyzed against pure water for 3 days.

^{1}H NMR (600 MHz, D_2O, δ): 3.36 (s, 3H, CH_3), 3.59−3.70 (m, 50H, CH_2, 2H, CH_2, H(3) and H(5) of alginate), 3.86 (s, H(2) and H(4) of alginate), 4.31 (s, 2H, CH_2). The ^{1}H NMR spectrum of Alg-*g*-PEG is shown in Figure S3. The PEG content was calculated from the peak integration of the ^{1}H spectrum.

^{13}C NMR (600 MHz, D_2O, δ): 70.0 ± 3.0 (s, CH_2 of PEG, and C(3) of the G residues of alginate), 60.4 (CH_3 of PEG), 106.0 (C(1) of the M residues of alginate), 100.1 (C(1) of the G residues of alginate), 80.6 (C(4) of the G residues of alginate), 77.9 (C(4) of the M residues of alginate), 75.1 (C(3) and C(5) of the M residues of alginate), 66.3 (C(5) of the G residues of alginate), 65.2 and 65.7 (C(2) of alginate). The ^{13}C NMR spectrum of Alg-*g*-PEG is shown in Figure S4.

2.3. Preparation of Hollow Nanospheres. As an example, the preparation of Alg-g-PEG/α-CD aggregation is described: an Alg-*g*-PEG aqueous solution (pH 8) (1% w/v, 2 mL) was added dropwise to an α-CD saturated aqueous solution (3 mL) under stirring. With the addition of Alg-*g*-PEG, the solution became turbid, which indicated the formation of nanospheres. The resultant solution was dialyzed against pure water for 1 day to remove excess α-CD at 17 °C. To prepare samples for transmission electron microscopy (TEM) and atomic force microscopy (AFM), one drop of the diluted solution was cast on a carbon-coated copper grid (for TEM) or a mica wafter (for AFM).

2.4. Measurements. The ^{1}H and ^{13}C NMR spectra were recorded on an Advance Bruker 600 NMR spectrometer at 600 MHz at room temperature. Thermogravimetric analyses (TGA) were undertaken using a TA Instruments Q500. Samples were heated at 10 °C/min from room temperature to 500 °C in a dynamic nitrogen atmosphere with a flow rate of 70 mL/min. TEM observations were performed on a Jeol JEM-100CX electron microscope at an accelerating voltage of 80 kV. AFM measurements were performed on a Nanoscope Multimode SPM with a Nanoscope IIIa controller (Vecco Instruments, U.S.). The images were taken in tapping mode. The hydrodynamic diameter (D_h) of the particles was measured by dynamic light scattering (DLS). DLS measurements were carried out on Brookhaven BI-200SM equipment at a wavelength of 532 nm and a scattering angle of 90°. The crystalline changes in the hollow nanospheres were confirmed by X-ray diffraction measurements, which were performed by using Cu Kα irradiation with a Philips X'Pert MPD (20 kV, 35 mA, 2°/min). The zeta potential of Alg-*g*-PEG/α-CD hollow spheres was measured using a Zetasizer model Nano-ZS (Malvern Instruments, England).

3. RESULTS AND DISCUSSION

3.1. Synthesis of Alg-*g*-PEG. Sodium alginate has been extensively studied as a biocompatible, biodegradable, water-soluble natural polysaccharide for biomedical applications.[23,24] To fabricate hollow spheres with good biocompatibility, we chose Alg-*g*-PEG, the derivative of alginate, to construct a rigid-coil system. Alg-*g*-PEG was synthesized by bonding PEG oligomers on the alginate backbone. ^{1}H NMR (Figure S3), ^{13}C

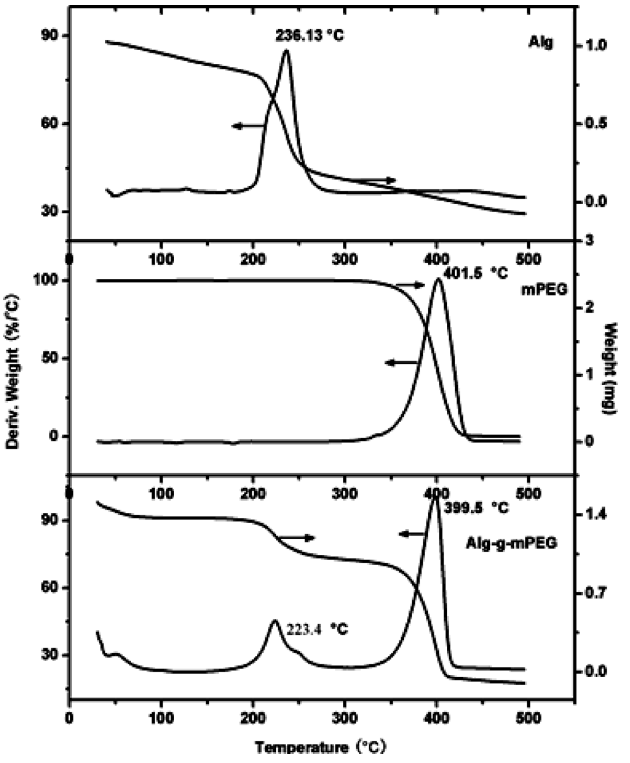

Figure 1. TGA thermograms of alginate, PEG, and Alg-*g*-PEG/α-CD.

NMR (Figure S4), and TGA (Figure 1) confirmed the formation of Alg-*g*-PEG. Because the decomposition temperature interval of the Alg and mPEG components is significant, the PEG graft density can be calculated using eqs 1 and 2. Table 1 lists Alg-*g*-PEG samples with different graft densities or molecular weights of PEG.

$$\text{percentage of Alg component } W, W = \frac{W_1}{(1 - W_2) \times 51.82\%} \times 100\% \quad (1)$$

where W_1 is the Alg component of Alg-*g*-PEG loss between 120 and 320 °C, W_2 is the moisture loss, and 51.82% is the pure Alg loss between 120 and 320 °C.

$$\text{PEG graft density (GD), GD} = \frac{198 \times W}{\text{average molecular weight of mPEG} \times (1 - W)} \times 100\% \quad (2)$$

where 198 is the molar mass of the Alg unit.

3.2. Self-Assembly of α-CD and Alg-*g*-PEG into Hollow Spheres. When aqueous solutions of α-CDs were mixed with a transparent aqueous solution of Alg-*g*-PEG at room temperature, the solution gradually became slightly turbid, indicating the formation of some kind of aggregates. The morphology of the aggregates was studied by TEM and AFM (at 17 °C, pH 7). Figure 2 shows the typical morphologies of Alg-*g*-mPEG (sample 5)/α-CD particles. It can be seen that there is an obvious contrast between the central and outer parts of a particle (Figure 2A), which was a typical TEM image of hollow spheres.[14−20] The AFM micrograph (Figure 2B) showed that the aggregates are spherical in shape. The horizontal distance was 234 nm, but the

Table 1. Synthesis Results of Alg-*g*-PEG

sample	M_w of NH_2−PEG	PEG graft density (%)[a]
1	1000	21.25
2	2000	65.67
3	2000	57.04
4	2000	26.43
5	2000	15.60
6	2000	7.62
7	5000	27.69

[a] The PEG content in Alg-*g*-PEG calculated from TGA.

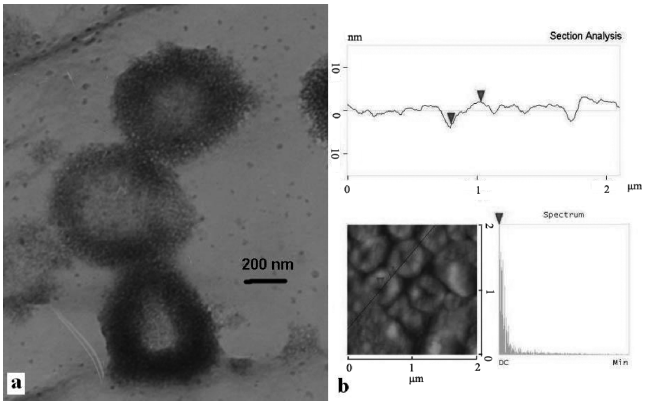

Figure 2. (a) TEM image of the Alg-*g*-PEG (sample 5)/α-CD particle. (b) AFM image of the Alg-*g*-PEG (sample 5)/α-CD particles.

vertical distance was 5 nm. As reported for AFM observations, such remarkable size differences between the horizontal and vertical directions of spheres were always attributed to hollow structures.[25]

CDs are well known in supramolecular chemistry as host compounds capable of including a range of guest molecules in their cavities with high selectivity.[26,27] It has been reported that the PEG chain was used to form a PEG-α-CD inclusion complex with α-CD in water, and the resulting rod-like crystallites were water-insoluble because the adjacent α-CD molecules packed closely through hydrogen bonding.[28−31] Alg-*g*-PEG was expected to form inclusion complexes with α-CD because of the existence of PEG grafts, although the alginate backbone was too large to penetrate the cavity of α-CD. Figure 3d shows a typical XRD pattern of the Alg-*g*-mPEG/α-CD hollow spheres. It can be seen that the pattern of Alg-*g*-mPEG/α-CD shows a strong reflections at $2\theta = 19.9°$, which are different from those of free Alg-*g*-mPEG and α-CD but very similar to that of PEG-α-CD. ^{1}H NMR analysis showed that the stoichiometry of [EG] to [α-CD] in Alg-*g*-mPEG/α-CD aggregates was about 2:1 (a typical ^{1}H NMR spectrum of Alg-*g*-mPEG/α-CD is shown in Supporting Information Figure S5), which matched well with the case of complete PEG-α-CD inclusion complexes.[28,29] This result indicated that Alg-*g*-mPEG/α-CD also contained PEG-α-CD inclusion crystals, in which the α-CD rings are stacked along the grafted PEG chain to form a rod-like structure. As a result, the Alg-*g*-mPEG/α-CD complexes have both a rod block (PEG-α-CD inclusion) and a coil block (protonated Alg backbone).

Jenekhe et al. and Jiang et al. have reported that the rod-like block in the rod−coil system preferred parallel packing crowdedly and

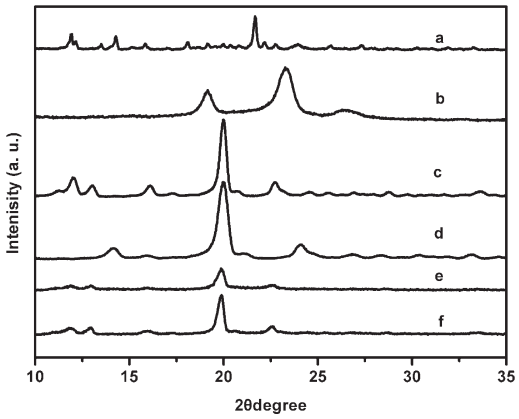

Figure 3. XRD patterns of (a) α-CD, (b) Alg-*g*-PEG, (c) a complete PEG-α-CD (PEG M_w = 1000) inclusion complex, (d) Alg-*g*-PEG/α-CD (sample 5/α-CD, pH 7), (e) Alg-*g*-PEG/α-CD (sample 5/α-CD, pH 3), and (f) Alg-*g*-PEG/α-CD (sample 5/α-CD, pH 11).

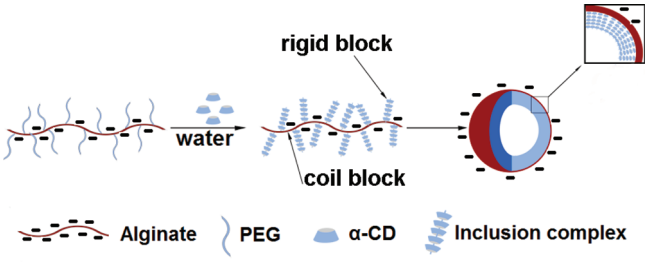

Figure 4. Schematic illustration of the formation of the Alg-*g*-PEG/α-CD hollow sphere.

resulted in the formation of hollow spheres that are necessary to efficient space-filling packing.[14−20] Taking these reports into account, the mechanism of the aggregation of Alg-*g*-mPEG/α-CD complexes is proposed as Figure 4: in the aqueous solution, α-CD molecules were threaded onto PEG chains to form a rod-like segment, and the simultaneously protonated alginate backbone acted as a coil block. The requirement of efficient space-filling packing of the rod-like block resulted in the PEG-α-CD inclusions preferring the pack radially into a sphere to form a hollow structure. The expected structure of such an aggregate is an inner PEG-α-CD inclusion surrounded by the protonated alginate shell. The zeta potentials of all of the Alg-*g*-mPEG/α-CD particles were around −26 mV (−26.2 ± 0.6 mV), confirming that the surfaces of Alg-*g*-mPEG/α-CD particles were covered with protonated alginate segments.

Harada et al. reported that the addition of urea resulted in the solubilization of the PEG-α-CD inclusion complexes because hydrogen bonding between α-CDs was attenuated.[28,29] In our experiments, the effect of urea on the formation of hollow spheres was investigated by measuring the transmittance of the mixed solution of urea and Alg-*g*-mPEG/α-CD. The results are shown in Figure 5. It can be seen that the solution without urea became turbid within 60 min but the addition of urea led to the solution remaining transparent even after 600 min. The solution with more urea showed a higher transmission. These results indicated that the Alg-*g*-mPEG/α-CD particles were disintegrated with the addition of urea and suggested that the crystalline aggregation of PEG and α-CD played an essential role in the formation of Alg-*g*-mPEG/α-CD spheres.

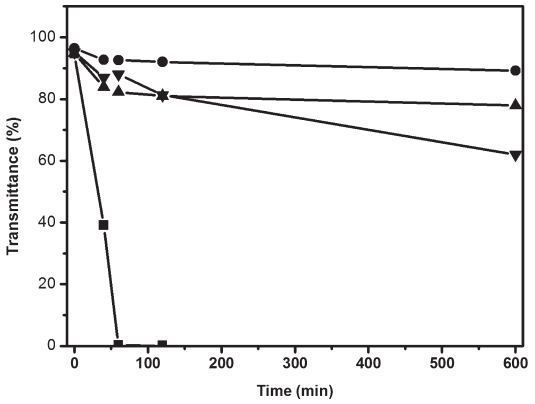

Figure 5. Transmittance of the Alg-*g*-PEG/α-CD (sample 5/α-CD) and urea mixed solution at 17 °C. (●) Sample 1 (OH (α-CD): NH_2 (urea) = 1:2; (▲) sample 2 (OH (α-CD): NH_2 (urea) = 1:1; (▼) sample 3 (OH (α-CD): NH_2(urea) = 1:0.6; (■) sample 4 without urea.

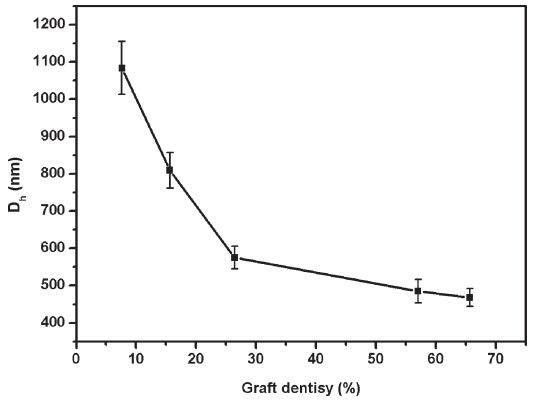

Figure 6. D_h of Alg-*g*-PEG/α-CD hollow spheres with different PEG graft densities.

3.3. Effect of the Graft Density and Molecular Weight of PEG on the Self-Assembly of Alg-*g*-PEG/α-CD. To evaluate the influence of the PEG graft density on the self-assembly of Alg-*g*-PEG/α-CD, we synthesized a series of Alg-*g*-PEG with different graft density using mPEG2000 (M_w = 2000) and prepared Alg-*g*-PEG/α-CD using these samples at 17 °C. The AFM results of these Alg-*g*-PEG/α-CD aggregates (Figure S6) were quite analogous to those of Alg-*g*-PEG(sample 5)/α-CD hollow particles (Figure 2b), which were spherical in shape and remarkable different in size between the horizontal and vertical directions of spheres, suggesting that all of the Alg-*g*-PEG/α-CD aggregates contained a hollow cavity and the shells collapsed into highly flattened objects after deposition on substrates.

As shown in Figure 6, the D_h of Alg-*g*-PEG/α-CD particles apparently decreased with increases in the PEG graft density. Meanwhile, the particles displayed a more broad distribution when the graft density decreased to 7.62%. As discussed before, the grafted PEG penetrated the inner cavity of α-CD to form a rod-like inclusion during the self-assembly process of Alg-*g*-PEG and α-CD. A high PEG graft density should result in a high content of rod-like water-insoluble block formation in Alg-*g*-PEG/α-CD complexes. It seems that the large density of rod-like grafts favors the formation of small aggregates and promote the fine dispersion. This trend in the particle size varying with the

Table 2. D_h of Alg-*g*-PEG/α-CD Particles[a]

Alg-*g*-PEG/α-CD particles	M_n of PEG	graft density	D_h (nm)
sample 1/α-CD	1000	21.45	974
sample 4/α-CD	2000	26.43	659
sample 7/α-CD	5000	27.69	487

[a] All of the samples were prepared at 17 °C, and the copolymer concentration was 1%.

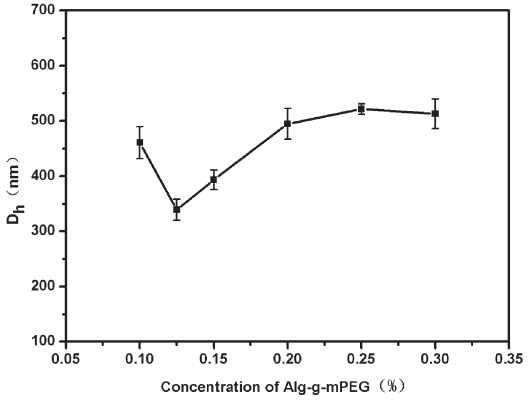

Figure 7. D_h of Alg-*g*-PEG/α-CD (sample 5/α-CD) hollow spheres with different assembly concentrations.

graft density of rod-like blocks is quite consistent with that reported for hollow spheres made from hydrogen-bonding graft copolymers.[16−20]

We also studied the effect of the length of PEG on the self-assembly of Alg-*g*-PEG and α-CD. It was found that the stoichiometry of [EG] to [α-CD] in Alg-*g*-mPEG/α-CD particles was all about 2:1 (calculated from ^{1}H NMR). This result indicated that the threading process was not changed when the length PEG changed and all of the PEG chains were covered by α-CDs to form a complete PEG-α-CD inclusion. Table 2 showed the D_h data of Alg-*g*-PEG/α-CD particles made from Alg-*g*-PEG copolymers having a similar graft density but different graft chain lengths. It can be seen that the D_h of particles decreased as the length of PEG increased, which may be due to the fact that long PEG chains resulted in the Alg-*g*-PEG/α-CD complexes containing a high content of rod-like blocks.

On the basis of the analysis above, we could conclude that more rod-like blocks in Alg-*g*-PEG/α-CD favor the formation of small particles.

3.4. Effect of the Concentration on the Self-Assembly of Alg-*g*-PEG/α-CD. Figure 7 shows the D_h of Alg-*g*-PEG/α-CD as a function of concentration. Above 0.125%, the D_h of Alg-*g*-PEG/α-CD increased first as the concentration increased, which may be because the aggregation number of particles increased as the concentration increased. However, as the concentration increased further, the particle size gradually remained stable. It should be noticed that a significant increase in particle size occurred when the concentration was below 0.125%. Meanwhile, Alg-*g*-PEG/α-CD displayed a rather broad distribution. Structures with a large size (around 6−7 μm) and a small size (around 100 nm) both appeared in this system, indicating that the aggregates have a less homogeneous size and shape. At a concentration of 0.075%, the Alg-*g*-PEG/α-CD solution became transparent and no particles could be detected using DLS. The

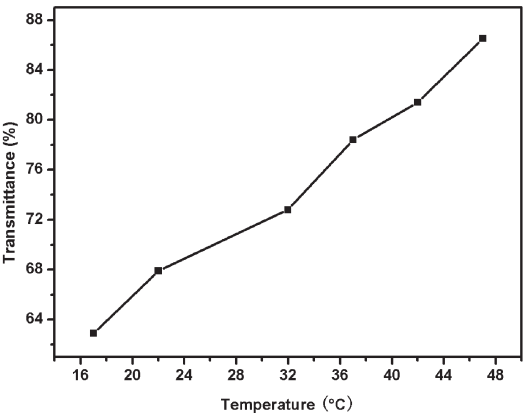

Figure 8. Transmittance of Alg-*g*-PEG/α-CD (sample 5/α-CD) as a function of temperature.

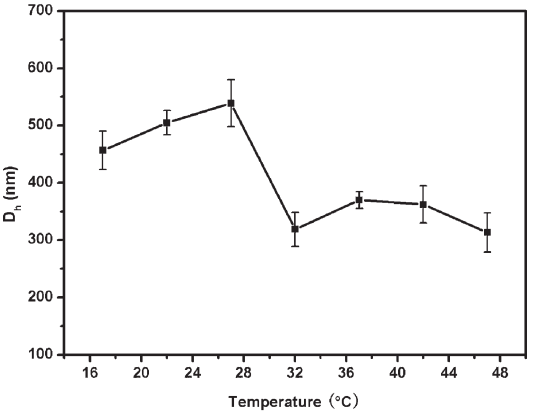

Figure 9. D_h of Alg-*g*-PEG/α-CD (sample 5/α-CD) as a function of temperature.

behavior implied that the assemblies of Alg-*g*-PEG/α-CD were stable and disrupted at low concentration.

3.5. Effect of Temperature on the Self-Assembly of Alg-*g*-PEG/α-CD. It is known that the temperature plays an important role in the formation of inclusions between CDs and polymers.[32−35] There is an inclusion−dissociation equilibrium between CDs and polymer chains in the inclusion complex formation process. Because the dissociation of CDs from the polymer chain is active when the polymer chain has a high mobility, inclusion formation is always favored by low temperature.

In our study, we measured the transmittance of Alg-*g*-PEG/α-CD solution as a function of temperature. It can be seen that the transmittance of the solution increased when the temperature increased (Figure 8), which implied that lots of Alg-*g*-PEG/α-CD particles were disrupted at high temperature. As we demonstrated before, the formation of PEG-α-CD played an essential role in the aggregation of Alg-*g*-mPEG/α-CD, so the disruption of Alg-*g*-mPEG/α-CD particles at high temperature was assigned to the dissociation of PEG-α-CD.

Figure 9 shows the D_h of Alg-*g*-mPEG/α-CD at different temperatures. It is interesting that D_h increased slowly at 17−27 °C but obviously decreased when the temperature increased to 32 °C. AFM and TEM studies demonstrated that the morphology of complexes was very similar at low temperature (7−27 °C) but as the temperature increased above 32 °C

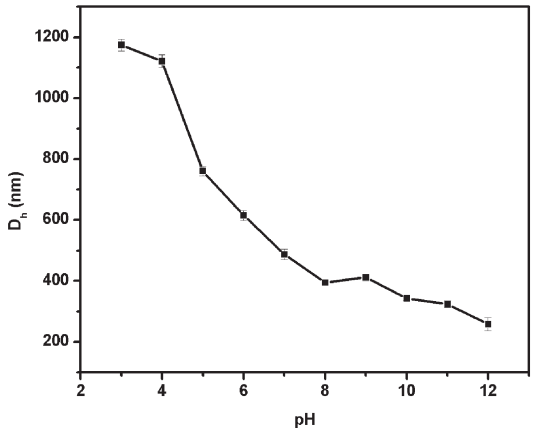

Figure 10. D_h of Alg-*g*-PEG/α-CD (sample 5/α-CD) as a function of pH.

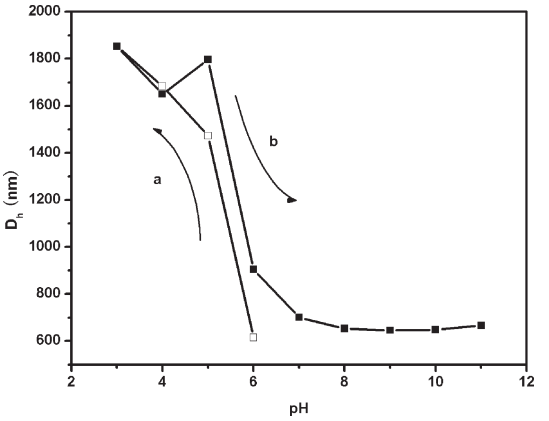

Figure 11. D_h of Alg-*g*-PEG/α-CD (sample 5/α-CD) as the pH is changing.

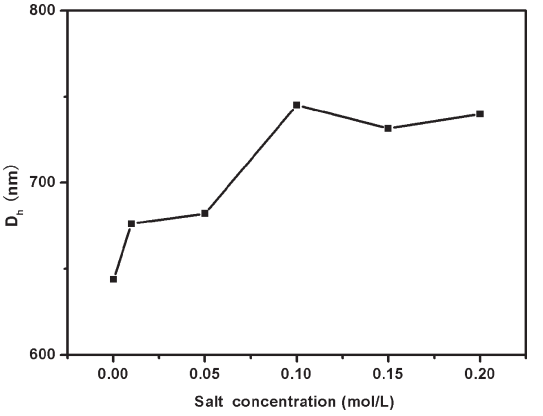

Figure 12. D_h of Alg-*g*-PEG/α-CD (sample 5/α-CD) as a function of salt concentration.

clear TEM and AFM images of samples became harder to obtain. Instead of hollow particles, large membrane-like structures with very few hollow particles were observed. (Typical TEM and AFM images of sample 5/α-CD are shown in Figure 2.)

The above phenomenon may be the result of two different effects: (1) Because increasing temperature resulted in the dissociation of rod-like PEG-α-CD, the rod-like block content in Alg-*g*-mPEG/α-CD decreased. As we discussed before, less rod-like block content led to increases in particle size. (2) As the temperature increased further (above 32 °C), the rod-like block decreased to very small proportion. As a consequence, the small portion of rod-like grafts was not enough to make all Alg-*g*-mPEG chains form large aggregates. Soluble, small Alg-*g*-mPEG/α-CD complexes formed. Similarly, in hydrogen-bonding graft copolymer systems, there were also soluble individual graft copolymers existing in the solution when the rod graft portion was low.[18]

3.6. Effect of pH on the Self-Assembly of Alg-*g*-PEG/α-CD. The D_h of Alg-*g*-mPEG/α-CD also showed a dependence on pH. Figure 10 shows the variation of Alg-*g*-mPEG/α-CD as the pH values decrease. At pH 3, the Alg-*g*-mPEG/α-CD showed structure with $D_h > 1$ μm. Meanwhile, few very large aggregates ($D_h = 7$ to 8 μm) also existed in this system. As the pH value increased from 3 to 8, the D_h of Alg-*g*-mPEG/α-CD decrease gradually and the large aggregates disappeared in this process. However, as the pH value decreased further, D_h did not change obviously.

It is well known that the alginate chains changed from less-soluble hypercoil chains to soluble extended chains as the pH value increased. In the low-pH region, the alginate chains were poorly soluble because of the protonation of carboxyl groups. Therefore, the Alg-*g*-mPEG/α-CD complexes were not stable and macrocosmic precipitation took place. As the pH value increased, the carboxyl groups ionized and then Alg-*g*-mPEG/α-CD became more and more stable. The alginate chains became totally hydrophilic because the carboxylic acid in the alginate chains ionized completely. Consequently, Alg-*g*-mPEG/α-CD formed stable hollow spheres, but it should be noted that we obtained only the AFM and TEM micrographs of the Alg-*g*-mPEG/α-CD complex (Figure 2) at pH 7 (which confirmed the hollow structures of Alg-*g*-mPEG/α-CD) because the morphology of the complex was covered by acid or alkali at other pH values.

Whether at pH 3 or 11, the pattern of the Alg-*g*-mPEG/α-CD complex showed a typical PEG-α-CD peak at 2θ = 19.9° (Figure 2e,f), which demonstrated that the PEG-α-CD inclusion was stable during the process of the pH changing. The pH dependence of Alg-*g*-mPEG/α-CD resulted only from the change in the alginate chains.

The pH dependence of Alg-*g*-mPEG/α-CD was also found to be reversible, but it should be noticed that the D_h value was larger than the original one when the pH value of the solution was adjusted to 6 again (Figure 11). This discrepancy could be caused by a difference in the salt concentration between the solutions. To confirm this argument, we investigated the effect of salt on the D_h of Alg-*g*-mPEG/α-CD.

3.7. Effect of Salt on the Self-Assembly of Alg-*g*-PEG/α-CD. As shown in Figure 12, the D_h of Alg-*g*-mPEG/α-CD increased with the salt concentration increasing (the salt was changed after the Alg-*g*-PEG/α-CD preparation), which may be caused by the salting-out effect on the alginate chains. As the salt concentration increased, the high ionic strength caused the solubility of alginate to decrease. Therefore, the van der Waals hydrophobic attractive forces between Alg chains resulted in the aggregation of Alg-*g*-mPEG/α-CD particles, as detected by the increase in the recorded D_h.

4. CONCLUSIONS

We presented a novel, convenient approach to hollow spheres. The strategy for fabrication was based on the self-assembly of rod−coil complexes, in which the rod-like segments were formed

by host/guest inclusion. More rod-like segments favor the formation of small particles. The concentration, temperature, pH, and salt greatly influence the self-assembly.

■ ASSOCIATED CONTENT

Supporting Information. Spectra of PEG-branched alginate. This material is available free of charge via the Internet at http://pubs.acs.org.

■ AUTHOR INFORMATION

Corresponding Author

*Tel: +86-28-85223843. Fax: (+86)28-85223843. E-mail: libj@cib.ac.cn (B.-J.L.). Tel, Fax: +86-28-85400266. E-mail: zslbj@163.com (S.Z.).

■ ACKNOWLEDGMENT

This work was financed by the National Natural Science Foundation of China (NSFC grant nos. 51073107, 21074138, and 50703025), CAS Knowledge Innovation Program (grant no. KSCX2-EW-J-22), Program for Changjiang Scholars, Innovative Research Team in University of Ministry of Education of China (IRT1026), and the Opening Project of the State Key Laboratory of Polymer Materials Engineering (Sichuan University KF201003).

■ REFERENCES

(1) Meier, W. *Chem. Soc. Rev.* **2000**, *29*, 295.
(2) Rösler, A.; Vandermeulen, G. W.; Klok, H. A. *Adv. Drug Delivery Rev.* **2001**, *53*, 95.
(3) Bergbreiter, D. E. *Angew. Chem., Int. Ed.* **1999**, *38*, 2870.
(4) Hu, Y.; Jiang, X. Q.; Din, Y.; Chen, Q.; Yang, C. Z. *Adv. Mater.* **2004**, *16*, 933.
(5) Shi, Z. Q.; Zhou, Y. F.; Yan, D. Y. *Macromol. Rapid Commun.* **2006**, *27*, 1265.
(6) Breitenkamp, K.; Emrick, T. *J. Am. Chem. Soc.* **2003**, *125*, 12070.
(7) Sanji, T.; Nakatsuka, Y.; Ohnishi, S.; Sakurai, H. *Macromolecules* **2000**, *33*, 8524.
(8) Wang, M.; Jiang, M.; Ning, F. L.; Chen, D. Y.; Liu, S. Y.; Duan, H. W. *Macromolecules* **2002**, *35*, 5980.
(9) Dou, H. J.; Jiang, M.; Peng, H. S.; Cheng, D. Y.; Hong, Y. *Angew. Chem., Int. Ed.* **2003**, *42*, 1516.
(10) Wang, J.; Jiang, M. *J. Am. Chem. Soc.* **2006**, *128*, 3703.
(11) Baidu, M. Y.; Cheng, Y. J.; Wickline, S. A.; Xia, Y. N. *Small* **2009**, *5*, 1747.
(12) Caruso, F.; Caroso, R. A.; Moehwald, H. *Science* **1998**, *282*, 1111.
(13) Xu, X.; Asher, S. A. *J. Am. Chem. Soc.* **2004**, *126*, 7940.
(14) Jenekhe, S. A.; Chen, X. L. *Science* **1999**, *283*, 372.
(15) Jenekhe, S. A.; Chen, X. L. *Science* **1998**, *279*, 1903.
(16) Duan, H. W.; Chen, D. Y.; Jiang, M.; Gan, W. J.; Li, S. J.; Wang, M.; Gong, J. *J. Am. Chem. Soc.* **2001**, *123*, 12097.
(17) Kuang, M.; Duan, H. W.; Wang, J.; Chen, D. Y.; Jiang, M. *Chem. Commun.* **2003**, 496.
(18) Duan, H. W.; Kuang, M.; Wang, J.; Chen, D. Y.; Jiang, M. *J. Phys. Chem. B* **2004**, *108*, 550.
(19) Kuang, M.; Duan, H. W.; Wang, J.; Jiang, M. *J. Phys. Chem. B* **2004**, *108*, 16023–16029.
(20) Chen, D. Y.; Jiang, M. *Acc. Chem. Res.* **2005**, *38*, 494.
(21) Meng, X. W.; Qin, J.; Liu, Y.; Fan, M. M.; Li, B. J.; Zhang, S.; Yu, X. Q. *Chem. Commun.* **2010**, *46*, 643.
(22) Ha, W.; Meng, X. W.; Li, Q.; Fan, M. M.; Peng, S. L.; Ding, L. S.; Tian, X.; Zhang, S.; Li, B. J. *Soft Matter* **2010**, *6*, 1405.
(23) Eiselt, P.; Lee, K. Y.; Mooney, D. J. *Macromolecules* **1999**, *32*, 5561.
(24) Hong, H. J.; Jin, S. E.; Park, J. S.; Ann, W. S.; Kim, C. K. *Biomaterials* **2008**, *29*, 4831.
(25) Huang, H. Y.; Remsen, E. E.; Kowalewski, T.; Wooley, K. L. *J. Am. Chem. Soc.* **1999**, *121*, 3805.
(26) Nepogodiev, S. A.; Stoddart, J. F. *Chem. Rev.* **1998**, *5*, 1959–1976.
(27) Wenz, G.; Han, B. H.; Muller, A. *Chem. Rev.* **2006**, *106*, 782.
(28) Harada, A.; Kamachi, M. *Macromolecules* **1990**, *23*, 2821–2823.
(29) Harada, A.; Li, J.; Kamachi, M. *Macromolecules* **1993**, *26*, 5698.
(30) Huang, L.; Allen, E.; Tonelli, A. E. *Polymer* **1998**, *39*, 4875.
(31) Zhang, S.; Yu, Z. J.; Govender, T.; Luo, H. Y.; Li, B. J. *Polymer* **2008**, *49*, 3205.
(32) Okumura, Y.; Ito, K.; Hayakawa, R. *Polym. Adv. Technol.* **2000**, *11*, 815.
(33) Ceccato, M.; LoNostro, P.; Baglioni, P. *Langmuir* **1997**, *13*, 2436.
(34) Yu, Z. J.; Liu, Y.; Fan, M. M.; Meng, X. W.; Li, B. J.; Zhang, S. *J. Polym. Sci., Part B: Polym. Phys.* **2010**, *48*, 951.
(35) Luo, H. Y.; Fan, M. M.; Yu, Z. J.; Meng, X. W.; Li, B. J.; Zhang, S. *Macromol. Chem. Phys.* **2009**, *210*, 669.